Proceedings of 10th International Coral Reef Symposium, 1727-1731 (2006)

Changing mangrove distributions in the Pioneer estuary (Queensland, Australia): evaluating a technique for monitoring mangrove health

Stacy JUPITER[1,2,3,*], Stuart PHINN[2], Norman DUKE[3] and Donald POTTS[1]

[1] Department of Ecology & Evolutionary Biology, University of California, 1156 High St, Santa Cruz, CA 95064, USA
[2] Centre for Remote Sensing and Spatial Information Science, School of Geography, Planning & Architecture, University of Queensland, St. Lucia, QLD 4072, Australia
[3] Centre for Marine Studies, University of Queensland, St. Lucia, QLD 4072, Australia
[*]Corresponding author: S. Jupiter
FAX: 1-831-459-5353, e-mail: jupiter@biology.ucsc.edu

Abstract The net area of mangroves in the Pioneer estuary (Queensland, Australia) has declined by 22% (137 ha) since 1948 due to clearing, development, hydrological manipulations, and climate variation. Within the past decade, a severe species-specific dieback has additionally affected over 50% of remnant mangrove cover within the system. We predict this recent, rapid mangrove loss has increased erosion of estuarine sediments and pollutants to nearshore waters. Quantifying historical mangrove changes in the Pioneer Estuary is the key for understanding potential threats to nearshore water quality. While manual digitization from aerial photography is suitable for mapping broadscale changes in mangrove distribution, this technique underestimates the total loss due to dieback. Regions of mangrove dieback can be mapped more effectively and efficiently by applying the Normalized Difference Vegetation Index (NDVI) to Landsat satellite data. In change detection analyses from 1990 to 2000, 44 ha had "lower NDVI" (i.e. reduced canopy density) and 56 ha had "higher NDVI" (i.e. increased canopy density). This study illustrates use of change detection analysis as an important monitoring tool for mangrove habitats in regions of heavy anthropogenic influence; its advantages include rapid processing time (hours), low data costs, and high accuracy.

Keywords Pioneer estuary, mangrove, dieback, aerial photography, Landsat, change detection analysis

Introduction

Models of changing sediment and nutrient flux into the Great Barrier Reef (GBR) Lagoon suggest loads have increased two to sixfold since the onset (~1850) of European land clearing (Furnas and Mitchell 2001; Neil et al. 2002). Because mangrove systems serve as a sink for suspended particles, adsorbed nutrients and associated pollutants (Tam and Wong 1995; Furukawa and Wolanksi 1996), changes in land use that impact mangrove distribution over time may have the potential to exert significant controls over nearshore water quality. Therefore, effects of mangroves in Queensland catchments such as the Pioneer, with its high sediment/nutrient exports and a net loss of mangroves over the past half-century (Duke and Wolanksi 2001), on the health status of adjacent marine ecosystems are matters of primary concern for management and conservation.

In addition to direct loss of mangroves from clearing and hydrological manipulations, the Pioneer estuary has recently experienced a severe mangrove dieback, most obviously affecting the normally broadly tolerant mangrove, *Avicennia marina* (Forssk.) Vierh. In live stands, *A. marina* pneumatophore density is correlated with sediment accretion (Young and Harvey 1996). Gaps created by *A. marina* death may reduce the sediment trapping capacity of the estuary and facilitate bank destabilization, as large *A. marina* dominate tidal creek margins. Additionally, death and root breakdown of dieback-affected trees may cause substantial sediment release into estuarine and nearshore waters in a process similar to that observed elsewhere following *A. marina* death from oil pollution (Duke and Burns 1997). The exported estuarine mud potentially threatens nearby coral reef health, since its resuspension causes aggregation of particles into sticky flocs that smother coral recruits and prevent recolonization after disturbance (Fabricius and Wolanski 2001).

Both aerial photographs (Dahdouh-Guebas et al. 2000; Lucas *et al.* 2002) and satellite imagery (Lara et al. 2002) have been used to map changes to mangrove ecosystems. Change detection analysis from satellite data has never before been applied to GBR Lagoon mangrove canopies affected by dieback, and the technique offers substantial advantages in the speed and ease of data processing. We used both historical aerial photographs and Landsat satellite data (Thematic Mapper (TM) and Enhanced Thematic Mapper (ETM)) to map changes in mangrove distribution through time (1948-2002) and to identify areas of mangrove dieback where significant

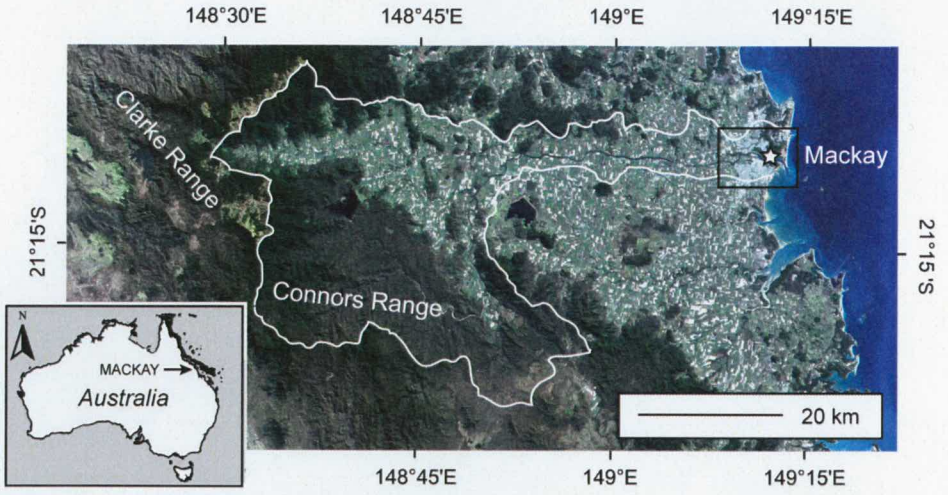

Fig. 1. Location of the city of Mackay, Queensland, Australia (inset) and within the Pioneer River catchment (white outline) depicted on a Landsat 7 ETM image, captured 16 July 2000. Mangroves of the Pioneer estuary surround the city of Mackay. Dark green indicates remnant native vegetation, while light green indicates land cleared for sugarcane cultivation.

export of estuarine mud may be occurring. Direct comparisons of these mangrove distribution changes with corresponding changes to nearshore water quality should provide evidence of the degree to which mangroves of the Pioneer estuary can buffer nearshore coral reefs from increasing river runoff. Results from this study are the first in a series that will examine linkages between catchment agricultural expansion, mangrove cover change and nearshore water quality change in the Pioneer catchment.

Study Site

The Pioneer catchment (Fig. 1; between 21° and 21° 25'S) covers 1570 km^2 near the central Queensland coast. Approximately 296 km^2 is used for sugarcane cultivation and 1166 km^2 is used mainly for grazing (GBRMPA 2001). Between 1930 to 1998, the area of sugarcane harvested from Mackay region mills increased by ~2000% (Canegrowers, personal communication). Runoff rates are enhanced by steep catchment topography, easily eroded soils and high annual rainfall (mean = 1385 mm/yr) (GBRMPA 2001). Most of the discharge and sediment deposition occurs in and around the Pioneer estuary, a complex multispecies system with at least 17 observed species of mangroves. Since 1948, tidal wetlands have been filled at ~5-6 ha/yr to support expanding urban pressures from Mackay, with a population of ~75,000 in 1998 and a 2.2% annual growth rate (Furnas 2003). *Avicennia marina* grows in association with other species in approximately 57% of the total mangrove area, an estimated 97% of which has been affected by moderate to severe dieback (Duke et al. 2005).

Methods

Mapping mangrove change through time

Black and white (1948; 1:30,000) and color (2002; 1:100,000) aerial photographs covering the Pioneer River estuary and the city of Mackay, Queensland (Fig. 1) were borrowed from the Marine Botany Group at the University of Queensland. Individual photographs were scanned at 600 dpi, mosaicked and georeferenced to part of a Landsat ETM image captured on 16 July 2000 using ENVI 3.6 software. Mangrove distributions were digitized based on *a priori* field knowledge and their contrast with adjacent substrates using ArcView 3.2 software. Distributions were categorized as tidal, non-tidal and new growth. All changes are reported relative to the 1948 baseline.

Change detection analysis from satellite data

The Pioneer estuary subset of the 2000 ETM image (16 July 2000) was radiometrically matched to a 1990 TM image (24 April 2004) using an empirical line calibration to correct for differences in solar irradiance and atmospheric path radiance. A mask exposing the mangrove distribution within the Pioneer estuary was created by digitizing from the 2002 aerial photograph mosaic and then used to subset the estuary area from the corrected 1990 and 2000 Landsat images. The Landsat images were then used to produce vegetation index images for the Pioneer River estuary in 1990 and 2000. Vegetation index images of mangroves, particularly the normalized difference vegetation index (NDVI), are recognized as correlates of biomass, canopy cover and leaf area index (Green and Mumby 2000). The unitless NDVI (ranging from –1 to 1) was calculated from the equation: NDVI = (NIR – Red)/(NIR + Red), where NIR is the % reflectance in the near infrared (Landsat Band 4; 0.76-0.90 μm) and Red is the % reflectance in the visible red (Landsat Band 3; 0.63-0.69 μm). A difference image was then calculated: Difference = ($NDVI_{1990}$ + 1) –

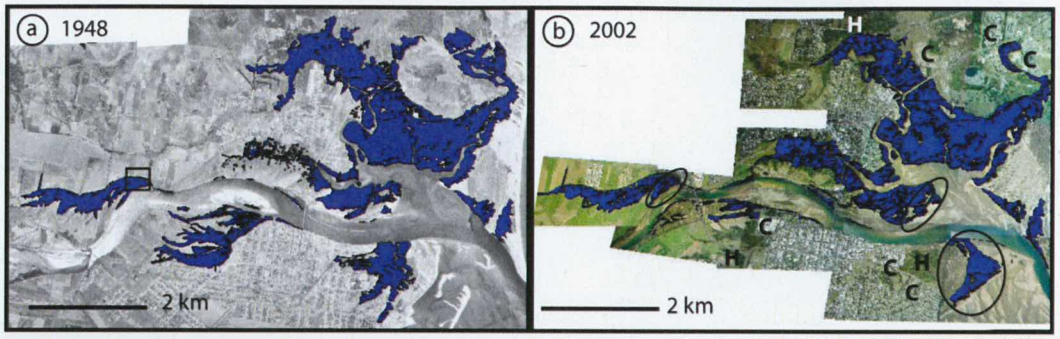

Fig. 2. Estuary-scale changes in Pioneer estuary mangrove distributions, 1948-2002, mapped from aerial photomosaics. (a) 1948 distribution of tidally flushed mangroves (blue). The black box identifies the focus region of Fig. 3. (b) 2002 distribution of tidally flushed mangroves (blue). C: major cleared regions. H: remnant mangroves restricted from tidal flushing . Circles: regions of new mangrove growth along river bends.

($NDVI_{2000}$ + 1), with 1 added to all NDVI values to avoid the subtraction of negative values. Pixels within the difference image were classified as "lower NDVI" (< -0.05), "no change" (-0.05-0.30) or "higher NDVI" (>0.30).

We used a regression to test for significance between calculated NDVI values from the 2000 Landsat ETM image and field measurements of mangrove density (for all trees ≥ 1m; collected May 2003-March 2004) in 5 m x 5 m plots (n = 16). We assessed correlations between NDVI change classes and mangrove canopy density through a normalized 2 x 2 error matrix (Congalton 1991). Georeferenced aerial photographs from 1991 and 1998 (the two closest dates for which aerial photographs were available within the bounds (1990-2000) of the change detection analysis) served as reference images. One hundred and fifty points were selected for comparison using a stratified random sampling design. Paired points (1991, 1998) on the aerial photographs were visually assessed for increases or decreases in mangrove canopy density and compared against the calculated NDVI class. The error matrix reports the overall correlation between the NDVI map and reference data, as well as the user accuracy (the probability that a classified NDVI pixel correctly represents the mangrove density change observed from the aerial photographs) and the producer accuracy (the probability that any pixel has been correctly classified to its correct class) (Congalton 1991).

Results

Mangrove distribution change, 1948-2002

During 1948-2002, the total area of tidally flushed mangroves within the Pioneer estuary decreased by 22%, principally from anthropogenic activities such as clearing, filling and altering the natural hydrodynamic structure (Fig. 2). The breakdown of mangrove change attributed to clearing, hydrological manipulations and new growth is summarized in Table 1. Mangroves were cleared at an average rate of ~4 ha/yr for both

Table 1. Changes in mangrove distributions (ha) mapped from aerial photographs between 1948 and 2002.

	Tidally flushed	Cleared	Non-tidal	New growth
1948	634	--	--	--
2002	497	221	53	137

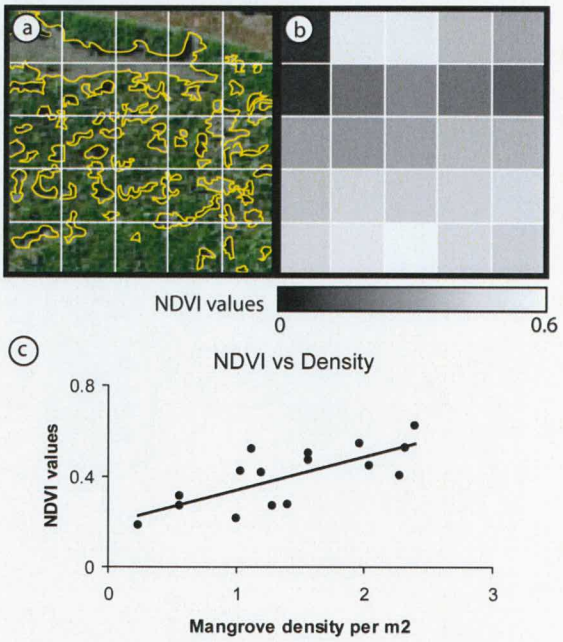

Fig. 3. Comparison of mangrove canopy maps derived from aerial photography and satellite data, and the NDVI relationship to canopy density. (a) Subset of a 2002 color aerial photograph in a region of substantial dieback. Canopy gaps from dieback are outlined in yellow. Each box represents the scale of one Landsat pixel (28.5m x 28.5m). (b) NDVI classification from 2000 Landsat ETM data for the same region. Brighter pixels have denser, greener mangrove canopy. Darker pixels are regions with greater open space. (c) NDVI values from the 2000 Landsat image plotted against mangrove tree density within 5 m x 5 m plots at each location.

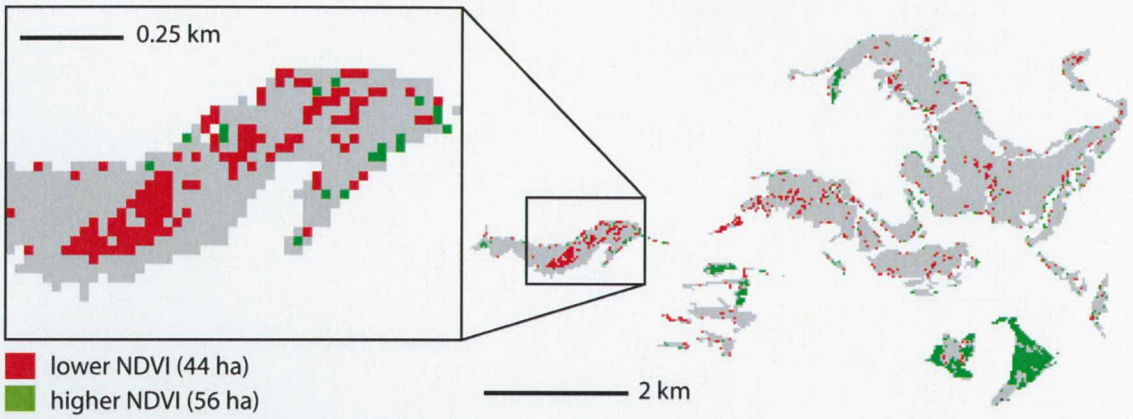

Fig. 4. Change detection analysis of NDVI change for 1990-2000. The high density of red pixels in Fursden creek (inset) match areas of heavy dieback (see Fig. 3).

agricultural and urban expansion. New highways, levees and a railway isolated patches of persistent, non-tidal mangroves that can no longer be counted among the total hectares available for filtration of runoff (Fig. 2b). The total loss of tidal mangroves (274 ha) was partially offset by 137 ha of new growth, particularly at river bends where decreased velocity has facilitated recent sediment deposition (Fig. 2b, black circles).

Distribution change from mangrove dieback

Mangrove dieback appears in aerial photographs as small canopy gaps with light brown areas of visible muddy substrate or as dark patches caused by tree shadow (Fig. 3a). Due to the labor required for complete and accurate digitization around every dieback gap, estuary-scale mapping of mangrove distribution from aerial photographs usually underestimates the magnitude of mangrove loss. Mangrove dieback, however, can be mapped more quickly from satellite imagery (hours *vs.* days). NDVI analysis applied to Landsat satellite data integrates the bare ground exposed by canopy gaps with mangrove cover across 28.5 m x 28.5 m image pixels. Pixels with thinner canopies (more dieback) resulted in lower NDVI values (Fig. 3b). The correlation between NDVI and field measurements of mangrove tree density was significant ($r^2 = 0.543$, $p < 0.001$) (Fig. 3c).

In the change detection analysis for 1990-2000, 44 ha had "lower NDVI" and 56 ha had "higher NDVI" in 2000 (Figure 4). Dieback was most pronounced around creek margins, where *Avicennia marina* trees are both numerous and large. Error analysis demonstrated a significant correlation (98% overall accuracy) between NDVI change and canopy density change as observed from aerial photographs (Table 2).

Discussion

If historical changes in nearshore water quality are directly linked to changes in mangrove distribution and health, then using remote sensing to map changes in mangrove distribution and condition can serve as a powerful management tool for early detection of threats to nearshore marine ecosystems. While digitization of mangroves from aerial photographs is effective for capturing broadscale changes in mangrove distributions, the addition of even simple vegetation indices, such as NDVI, can be used to monitor changes in mangrove condition through time and to target areas for restoration or remedial action before degradation of the estuarine buffer zone. Results of this study may be improved with higher spatial resolution data (e.g. Ikonos) that is more sensitive to smaller canopy gaps and/or hyperspectral imagery (e.g. Casi, HyMap) that may be used to identify tree stress prior to death.

Table 2. Error matrix for correlation between NDVI classes and canopy density changes. Data are the numbers (out of 150) of (Landsat-sized) pixels matched between the NDVI change detection image and the pair of aerial photomosaics (1991, 1998). The overall correlation accuracy is in bold text.

		Reference Data (aerial photographs)		
		lower canopy density	higher canopy density	User Accuracy
Classification Data (NDVI)	lower NDVI	59	2	96.7%
	higher NDVI	1	88	98.9%
	Producer Accuracy	98.3%	97.8%	***98.0%***

Acknowledgements

This research was supported through a Fulbright Postgraduate Award and a NASA Graduate Student Researchers Program Fellowship. We thank Karen Joyce for processing assistance.

References

Congalton RG (1991) A review of assessing the accuracy of classification of remotely sensed data. Remote Sensing of Environment 37: 35-46

Dahdouh-Guebas F, Verheyden A, De Genst W, Hettiarachch S, Koedam N (2000) Four decadal vegetation dynamics in Sri Lankan mangroves as detected from sequential aerial photography: a case study in Galle. Bulletin of Marine Science 67(2): 741-759.

Duke NC, Pinzón ZS, Prada MC (1997) Large-scale damage to mangrove forests following two large oil spills in Panama. Biotropica 29(1): 2-14

Duke NC, Wolanski E (2001) Muddy coastal waters and depleted mangrove coastlines. In: Wolanski E (ed) Oceanographic Processes of Coral Reefs: Physical and Biological Links in the Great Barrier Reef. CRC Press, Boca Raton, FL, pp 77-91

Duke, NC, Bell, AM, Pederson, DK, Roelfsema, CM, Bengston Nash, S (2005) Herbicides implicated as the cause of severe mangrove dieback in the Mackay region, NE Australia: consequences for marine plant habitats of the GBR World Heritage Area. Marine Pollution Bulletin 51: 308-324

Furnas, M (2003) Catchments and Corals. Australian Instriture of Marine Sciences, Townsville, Australia, 334 pp

Furnas M, Mitchell A (2001) Runoff of terrestrial sediments and nutrients into the Great Barrier Reef World Heritage Area. In: Wolanski E (ed) Oceanographic Processes of Coral Reefs: Physical and Biological Links in the Great Barrier Reef. CRC Press, Boca Raton, FL, pp 37-51

Furukawa K, Wolanski E (1996) Sedimentation in mangrove forests. Mangroves and Salt Marshes 1(1): 3-10.

GBRMPA (2001) Water quality action plan: a report to Ministerial Council on targets for pollutant loads. Great Barrier Reef Marine Park Authority, Townsville, 68 pp

Green EP and Mumby PJ (2000) Mapping Mangroves. In: Edwards AJ (ed) Remote Sensing Handbook for Tropical Coastal Management. UNESCO Publishing, Paris, pp 183-197

Lara R, Szlafsztein C, Cohen M, Berger U, Glaser M (2002) Implications of mangrove dynamics for private land use in Bragança, North Brazil: a case study. Journal of Coastal Conservation 8(1): 97-102

Lucas RM, Ellison JC, Mitchell A, Donnelly B, Finalyson M, Milne AK (2002) Use of stereo aerial photography for quantifying changes in the extent and height of mangroves in tropical Australia. Wetlands Ecology and Management 10: 161-175

Neil DT, Orpin AR, Ridd PV, Yu, B (2002) Sediment yield and impacts from river catchments to the Great Barrier Reef lagoon. Marine & Freswater Research 53: 733-752

Tam NFY, Wong YS (1995) Mangrove soils as sinks for wastewater-borne pollutants. Hydrobiologia 295: 231-241

Young BM, Harvey LE (1995) A spatial analysis of the relationship between mangrove (*Avicennia marina* var. *australasica*) physiognomy and sediment accretion in the Hauraki Plains, New Zealand. Estuarine, Coastal and Shelf Science 42: 231-246